



HAL
open science

Performance of meta-predictors for the classification of MED13L missense variations, implication of raw parameters.

Thomas Smol, Frederic Frenois, Sylvie Manouvrier, Florence Petit, Jamal Ghoumid

► To cite this version:

Thomas Smol, Frederic Frenois, Sylvie Manouvrier, Florence Petit, Jamal Ghoumid. Performance of meta-predictors for the classification of MED13L missense variations, implication of raw parameters.. European Journal of Medical Genetics, 2021, European Journal of Medical Genetics, 65, pp.104398. 10.1016/j.ejmg.2021.104398 . hal-04470913

HAL Id: hal-04470913

<https://hal.univ-lille.fr/hal-04470913v1>

Submitted on 22 Jul 2024

HAL is a multi-disciplinary open access archive for the deposit and dissemination of scientific research documents, whether they are published or not. The documents may come from teaching and research institutions in France or abroad, or from public or private research centers.

L'archive ouverte pluridisciplinaire **HAL**, est destinée au dépôt et à la diffusion de documents scientifiques de niveau recherche, publiés ou non, émanant des établissements d'enseignement et de recherche français ou étrangers, des laboratoires publics ou privés.



Distributed under a Creative Commons Attribution - NonCommercial 4.0 International License

Performance of meta-predictors for the classification of *MED13L* missense variations, implication of raw parameters

Thomas Smol^{1,2}, Frédéric Frénois^{1,3}, Sylvie Manouvrier-Hanu^{1,3}, Florence Petit^{1,3}, Jamal Ghoumid^{1,3}

¹ Université de Lille, EA7364 RADEME, F-59000, Lille, France

² CHU Lille, Institut de Génétique Médicale, F-59000, Lille, France

³ CHU Lille, Clinique de Génétique « Guy Fontaine », F-59000, Lille, France

Corresponding author

Jamal Ghoumid, M.D., PhD.

CHU Lille, Clinique de Génétique, Hôpital Jeanne de Flandre, F-59000 Lille

Tel: +33 3 20444911

Fax: +33 3 20444901

E-mail: jamal.ghoumid@chru-lille.fr

Conflict of interest

The authors declare no conflict of interest.

Abstract

MED13L syndrome is a rare congenital disorder comprising moderate intellectual disability, hypotonia and facial dysmorphism. Whole exome or genome sequencing in patients with non-specific neurodevelopmental disorders leads to identification of an increasing number of *MED13L* missense variations of unknown significance. The aim of our study was to identify relevant annotation parameters enhancing discrimination between candidate pathogenic or neutral missense variations, and to assess the performance of seven meta-predictor algorithms: BayesDel, CADD, DANN, FATHMM-XF, M-CAP, MISTIC and REVEL for the classification of *MED13L* missense variants. Significant differences were identified for five parameters: global conservation through verPhyloP and verPhCons scores; physico-chemical difference between amino acids estimated by Grantham scores; conservation of residues between MED13L and MED13 protein; proximity to phosphorylation sites for pathogenic variations. Among the seven selected *in-silico* tools, BayesDel, REVEL, and MISTIC provided the most interesting performances to discriminate pathogenic from neutral missense variations.

Individual gene parameter studies with *MED13L* have provided expertise on elements of annotation improving meta-predictor choices. The *in-silico* approach allows us to make valuable hypotheses to predict the involvement of these amino acids in *MED13L* pathogenic missense variations.

Key-words

***MED13L*; missense; conservation; *in-silico* algorithm; variant interpretation**

Introduction

In-silico predictive algorithms are now widely used for annotation of punctual variation in gene sequencing analysis. The American College of Medical Genetics and Genomics edited guidelines for proper use of these *in-silico* predictors [1]. Initially, first prediction strategies were based on either sequence/evolutionary conservation, or protein sequence, or supervised learning methods [2]. More complex approaches are now developed by combining multiple single tools [3]. These combinations, which define meta-predictors algorithms, often offer a continuous scoring rather than a 2-side classification. The vast majority of the studies compare the precision, accuracy and efficiency of *in-silico* tools on large multigene variation datasets such as the ClinVar database [4], and rarely focus on a specific gene for the classification of missense variants.

The *MED13L* syndrome is an autosomal dominant syndrome due to heterozygous pathogenic variations within *MED13L*, comprising moderate intellectual disability, hypotonia, and facial dysmorphism [5–10]. *MED13L* encode the subunit 13-like protein, member of the CDK8 module kinase, part of the mediator complex [11]. The first description of pathogenic variations involved either *de novo* heterozygous nonsense, or frameshift, or intragenic microdeletion assumed to lead to haploinsufficiency [5,7,8]. Interpretations of protein-truncating variations or recurrent missense variations identified in patients with typical phenotype will not cause any particular difficulties. However, whole exome or genome sequencing in patients with non-specific neurodevelopmental disorders leads to identification of an increasing number of *MED13L* missense variations of unknown signification [9,10,12–22].

The aim of our study was to identify relevant annotation parameters enhancing discrimination between candidate pathogenic or neutral missense variations, and to assess the performance of seven meta-predictor algorithms (BayesDel [23], CADD [3], DANN [24], FATHMM-XF

[25], M-CAP [26], MISTIC [27] and REVEL [28]) for the classification of known *MED13L* missense pathogenic variants.

Methods

Variation data and annotation

All possible combinations of *MED13L* missense variations were generated, corresponding to 14,545 different nucleotide substitutions. Missense variations were annotated with Ensembl Variant Effect Predictor (VEP), using genome assembly GRCh37, and with Combined Annotation Dependent Depletion (CADD), using version 1.3 [3,29]. We considered data parameters extracted from VEP and CADD annotations. Molecular anomalies with reported evidence of a splice defect, substitutions in the first or last three bases of each exon, were excluded from the analysis to prevent the pathogenicity classification associated with splice effect rather than pathogenicity due to an amino-acid substitution (n=398, 2.73%).

A comparison of conserved residues between MED13L and MED13 proteins was performed using Clustal Omega alignment with canonical transcript sequence of MED13L (Q71F56) and MED13 (Q9UHV7) obtained from Uniprot. Clustering was performed in R (v4.0.1). For each aligned amino acid, a score ranging from 0 to 1 was applied, according to the conservation of residues between MED13L and MED13. Fully conserved residues were annotated with the higher score “1”. Substitutions between two residues belonging to a group with strongly similar properties were annotated “0.5” and “0.25” respectively for groups with weakly similar properties. An unconserved substitution in the Gonnet PAM 250 matrix between MED13L and MED13 was annotated “0”. Distance to phosphorylation sites of each neutral or pathogenic missense on MED13L was estimated from PhosphoSite database on the protein model THRAP2, the previous name of MED13L [30].

Variations were classified according to ACMG 2015 criteria [1]. Frequencies of known reported alleles were considered using gnomAD, BRAVO, FREXAC and HGVD databases. Likely pathogenic and pathogenic variations described in the MED13L syndrome were identified in ClinVar, DECIPHER, HGMD and LOVD databases. Likely pathogenic and pathogenic variations previously reported were merged in the pathogenic missense group. Benign and likely benign missenses reported in ClinVar and LOVD, and missense variations above or equal to one allele in gnomAD control subpopulation, were merged in the control/neutral group.

Algorithms

Seven *in-silico* combined tools were used to analyze all the *MED13L* missense variants. All algorithms and methodology associated with the prediction tools are described in the reference articles. BayesDel is a deleteriousness measure, combining multiple annotation scores including PolyPhen2, SIFT, FATHMM, LRT, Mutation Taster, Mutation Assessor, PhyloP, GERP++, Siphy, and the minor allele frequency across populations [23]. BayesDel gave an important place to conservation measured and population frequency including ExAC [31]. CADD, Combined Annotation-Dependent Depletion, establishes a continuous Phred-like score from conservation matrix (GERP, PhastCons, PhyloP), functional annotations and protein-level scores (Grantham, SIFT, PolyPhen2) [3]. DANN, for deleterious annotation of genetic variants using neutral networks, is based on the same training data as CADD, but used a deep neural network rather a linear kernel support vector machine to score the variations [24]. FATHMM-XF scores are obtained from a supervised machine learning model using features from 27 data sets [25]. M-CAP, standing for Mendelian Clinically Applicable Pathogenicity Score, is notably based on pathogenicity scores as SIFT, PolyPhen2 and CADD [26]. MISTIC, for MISsense deleTeriousness predICTor, combines a soft voting system based

on Random Forest and Logistic Regression [27]. REVEL, for Rare Exome Variant Ensemble Learning, combines 9 individual tools: MutPred, FATHMM, VEST, PolyPhen2, SIFT, PROVEAN, Mutation Assessor, Mutation Taster and LRT, and 4 conservation scores: GERP, SiPhy, PhyloP and PhastCons [28]. To identify thresholds for *MED13L* gene variations for all tools, a logistic regression has been performed with OptimalCutpoints R package, with default parameters [32].

Performance comparison

For all algorithms, we calculated the overall accuracy (ACC), specificity, sensitivity and area under curve (AUC) from Receiver operating characteristics (ROC) curves. The positive predictive values (PPV) and the negative predictive values (NPV) were determined for each algorithm. The Matthews correlation coefficient (MCC) was used to provide a balanced comparison between *in-silico* tools. Comparison of pathogenic and neutral classifications was performed with the following R-packages: rstatix, mltools and pROC.

Results

Among the 14,545 missense variations, 38 were classified as pathogenic or likely pathogenic (0.26%) and 495 as benign or likely benign (3.42%). The descriptions of missenses are listed in supplemental table 1.

Comparison of annotation parameters

To identify relevant parameters, a comparison of 19 scores provided by VEP, and based on conservation, functional and protein-level annotations, was performed. Comparisons of features between the 495 control variations and the 38 pathogenic variations with statistically

significant differences were described Table 1. Statistically significant differences were identified for five parameters. Mean degree of physicochemical difference between pairs of amino acids estimated by Grantham scores was estimated at 58.00 [0.00 – 215.00] and at 94.50 [0.00 – 194.00] respectively for neutral and pathogenic variations ($p=5.31e-4$, *Wilcoxon test*). Significant differences in side chain atomic composition, polarity and size between the two amino acids were associated with missense pathogenic variations.

Analysis of conservation across the entire length of the MED13L protein was then performed. *MED13L* encodes a conserved protein associated with a global verPhyloP score of 3.30 [-2.87 – 6.53] over the entire protein sequence. Higher level of amino-acid and nucleotide conservations were observed for pathogenic variations compared to neutral variations with mean vertebrate verPhyloP scores respectively of 5.19 [0.17 – 6.17] and 3.04 [-0.84 – 6.32] ($p=1.14e-8$), as well as for verPhCons with mean scores of 1.00 [1.00 – 1.00] and 0.93 [0.00 – 1.00] ($p=5.17e-3$, *Wilcoxon test*). Therefore, MED13L appeared to be a conserved protein in which the more highly conserved amino acids could be involved in pathogenic variations.

Then, we compared the conservation between both MED13 and MED13L paralogs. Sequence alignments using Clustal Omega analysis allowed to identify a homology rate of 54.80% between the paralogs, and a high degree of conservation of amino-acids involved in pathogenic variations *versus* neutral variations: median values of 1.00 vs 0.50 ($p=2.95e-5$, *Wilcoxon test*). Only 4 out of the 38 pathogenic missenses involved “unconserved” amino acids in MED13 protein: p.(Pro573Leu), p.(Leu844Ile), p.(Ser878Phe) and p.(Pro879Leu). In MED13 protein sequence, the four amino acids corresponded respectively to Thr551, Ser810, Phe847, and Ser848 residues.

Then, we analyzed the proximity with a phosphorylation site for each missense variant. Indeed, phosphodegron motifs were previously identified in MED13L and MED13, and were found to be critical for their degradation and dissociation from the CDK8-module [33,34].

Pathogenic missense variations were significantly closer to phosphorylation sites than neutral missenses: 17.50 [0.00 – 263.00] vs 30.00 [0.00 – 321.00] ($p=2.95e-3$, *Wilcoxon test*). Twenty out of the 38 (52.6%) pathogenic missenses were identified within ± 20 amino acids of a phosphorylation site.

Evaluation of in-silico classification tool performance

As a first step, optimal cut-offs were determined for the seven *in-silico* tools which provide a global raw value. Using OptimalCutpoints R package, the thresholds were defined for BayesDel, CADD, DANN, FATHMM-XF, M-CAP, MISTIC and REVEL (Table 2). The performances of the *in-silico* evaluations were also described in Table 2. The ROC curves of the individual *in-silico* combined tools for *MED13L* showed that MISTIC presented the highest AUC with a 0.902 value (Figure 1A). The ACC scores ranked MISTIC, BayesDel and REVEL as the best tools with respectively values of 0.912, 0.902 and 0.886. Based on the MCC scores, MISTIC, BayesDel and REVEL provided the best performances with respectively values of 0.533, 0.492 and 0.484. Among the seven *in-silico* tools, MISTIC, REVEL, and BayesDel provided the most interesting performances to discriminate pathogenic from neutral missense variations.

Concordance analysis

Considering all reported pathogenic missense variations, we have assessed the level of correlation of all predictors. Only 18 out of the 38 pathogenic missense variations were classified as deleterious by all tools (47.4%). Twenty-five out of the 38 variations were considered as deleterious for at least 6 tools (65.8%). The correlations of the seven *in-silico* tools were then compared to predict the pathogenic and the neutral missense classifications. For pathogenic classifications, the strongest correlation was observed between BayesDel and

REVEL ($R^2 = 0.872$) (Figure 1D). For the neutral group, the strongest correlation was also observed between BayesDel and REVEL ($R^2 = 0.682$) (Figure 1C). Indeed, combination of BayesDel, REVEL and MISTIC showed the highest rate of correct prediction targeting pathogenic variations.

Discussion

Our study evaluated the performances of seven *in-silico* tools in order to evaluate *MED13L* missense classification, by targeting the most discriminant parameters. The ACMG/AMP guideline included the concordance of computational *in-silico* predictive programs in the criteria of variation classification, either with multiple lines of computational evidence for a deleterious effect on the gene, as PP3 criteria, or with multiple lines of computational evidence suggesting no impact on gene, as BP4 criteria [1]. When first reported *MED13L* pathogenic variations corresponded to *de novo* truncating variations as well as nonsense, frameshift, or intragenic deletions [5,7,8], the most recent now involve an important number of missense variations [9,10,35]. As the description of pathogenicity mechanisms in *MED13L* syndrome is still ongoing, the knowledge of *in-silico* missense annotations could improve performance in data interpretations, since computational parameters were routinely used in sequencing data analysis.

Based on all parameters evaluated, the verPhyloP scores have been considered as the most discriminant parameters with scores of 5.19 for pathogenic and 3.04 for neutral missenses ($p=1.14e-8$). The verPhyloP scores measured the evolutionary conservation at individual alignment sites in vertebrae [36]. *MED13L* is considered as a highly conserved protein across species with a global verPhyloP conservation score of 3.30 [11], and is involved in the

conserved CDK8 kinase module. However, some regions show higher conservation scores and are associated with clustering of *bona fide* pathogenic missense variations [9,35]. The importance of the conservation score was emphasized by the comparison between the two paralogs MED13 and MED13L [37]. We uncovered a strong association between amino acids involved in pathogenic missense variations and conserved residues, within MED13 and MED13L. These results would suggest a critical role played by these residues, whose function remains to be determined. The reciprocal is also observed within MED13. The five missense variations previously described in MED13-related neurodevelopmental disorder were highly conserved: p.(Thr326Ile), p.(Pro327Gln), p.(Pro327Ser), p.(Pro540Thr) and p.(Ala2064Val) (Supplemental Table 1) [34].

The physicochemical distance between two residues, evaluated by the Grantham score, is also considered as a robust parameter to discriminate pathogenic from neutral missense variations. The most frequently substituted amino-acids in pathogenic missenses were proline, serine, and threonine residues (43%, Supplemental Table 1). The recurrence of these three amino-acids in pathogenic substitutions could suggest an implication of MED13L phosphorylation sites [38]. One hypothesis could be an alteration of residues phosphorylated by proline-directed protein kinase targeting serine or threonine residues located next to a proline. Interestingly, CDK proteins, as well as CDK8, are members of the proline-directed serine/threonine-protein kinase family [39]. These residues could represent targets of cyclin C-CDK8 phosphorylation of MED13L altered in pathogenic missense variations [33].

Prediction of deleterious effect of *MED13L* missense variations using optimized thresholds showed relatively correct outcomes for the identification of potential neutral variations with negative predictive values ranging between 0.964 and 0.984 (Table 2). Conversely, as

expected, the positive predictive values were associated with the lowest scores, ranging from 0.132 for DANN to 0.441 for MISTIC (Table 2). Among the different *in-silico* tools, MISTIC, BayesDel and REVEL have outperformed other algorithms. The approach for MISTIC, with two different classes of machine-learning algorithms, including information of multiple conservation scores and functional measures, was associated with the highest scores for specificity, PPV, MCC, ACC and AUC (Table 2). Gene level evaluation using REVEL and BayesDel tools has previously considered one of the most discriminant *in-silico* tools for clinical variation classification considering actionable genes [40].

Our data highlighted the difficulty of the application of *in-silico* parameters in routine diagnosis when these global statistical approaches were applied to one gene targeting. Individual gene parameter studies, such as *MED13L*, provide expertise on elements of annotation improving meta-predictor choices. Moreover, the *in-silico* approach allows us to make useful hypotheses to predict the involvement of these amino acids in *MED13L* pathogenic missense variations.

Acknowledgements

We gratefully acknowledge the following: all members of the EA7364 RADEME team of Lille University for their comments; European Reference Network ITHACA for support.

References

- 1 Richards S, Aziz N, Bale S, Bick D, Das S, Gastier-Foster J, et al. Standards and guidelines for the interpretation of sequence variants: a joint consensus recommendation of the American College of Medical Genetics and Genomics and the Association for Molecular Pathology. *Genet Med Off J Am Coll Med Genet*. 2015 May;17(5):405–24.
- 2 Tavtigian SV, Greenblatt MS, Lesueur F, Byrnes GB, IARC Unclassified Genetic Variants Working Group. In silico analysis of missense substitutions using sequence-alignment based methods. *Hum Mutat*. 2008 Nov;29(11):1327–36.
- 3 Kircher M, Witten DM, Jain P, O’Roak BJ, Cooper GM, Shendure J. A general framework for estimating the relative pathogenicity of human genetic variants. *Nat Genet*. 2014 Mar;46(3):310–5.
- 4 Ghosh R, Oak N, Plon SE. Evaluation of in silico algorithms for use with ACMG/AMP clinical variant interpretation guidelines. *Genome Biol*. 2017 Nov;18(1):225.
- 5 Asadollahi R, Oneda B, Sheth F, Azzarello-Burri S, Baldinger R, Joset P, et al. Dosage changes of MED13L further delineate its role in congenital heart defects and intellectual disability. *Eur J Hum Genet EJHG*. 2013 Oct;21(10):1100–4.
- 6 Cafiero C, Marangi G, Orteschi D, Ali M, Asaro A, Ponzi E, et al. Novel de novo heterozygous loss-of-function variants in MED13L and further delineation of the MED13L haploinsufficiency syndrome. *Eur J Hum Genet EJHG*. 2015 Nov;23(11):1499–504.
- 7 van Haelst MM, Monroe GR, Duran K, van Binsbergen E, Breur JM, Giltay JC, et al. Further confirmation of the MED13L haploinsufficiency syndrome. *Eur J Hum Genet EJHG*. 2015 Jan;23(1):135–8.
- 8 Adegbola A, Musante L, Callewaert B, Maciel P, Hu H, Isidor B, et al. Redefining the MED13L syndrome. *Eur J Hum Genet EJHG*. 2015 Oct;23(10):1308–17.
- 9 Smol T, Petit F, Piton A, Keren B, Sanlaville D, Afenjar A, et al. MED13L-related intellectual disability: involvement of missense variants and delineation of the phenotype. *Neurogenetics*. 2018 Mar DOI: 10.1007/s10048-018-0541-0
- 10 Tørring PM, Larsen MJ, Brasch-Andersen C, Krogh LN, Kibæk M, Laulund L, et al. Is MED13L-related intellectual disability a recognizable syndrome? *Eur J Med Genet*. 2019 Feb;62(2):129–36.
- 11 Tsai K-L, Sato S, Tomomori-Sato C, Conaway RC, Conaway JW, Asturias FJ. A conserved Mediator-CDK8 kinase module association regulates Mediator-RNA polymerase II interaction. *Nat Struct Mol Biol*. 2013 May;20(5):611–9.
- 12 Bowling KM, Thompson ML, Amaral MD, Finnila CR, Hiatt SM, Engel KL, et al. Genomic diagnosis for children with intellectual disability and/or developmental delay. *Genome Med*. 2017 May;9(1):43.
- 13 Aoi H, Mizuguchi T, Ceroni JR, Kim VEH, Furquim I, Honjo RS, et al. Comprehensive genetic analysis of 57 families with clinically suspected Cornelia de Lange syndrome. *J Hum Genet*. 2019 Oct;64(10):967–78.

- 14 Ziats MN, Ahmad A, Bernat JA, Fisher R, Glassford M, Hannibal MC, et al. Genotype-phenotype analysis of 523 patients by genetics evaluation and clinical exome sequencing. *Pediatr Res.* 2020 Mar;87(4):735–9.
- 15 Geldon L, Mackenroth L, Kahlert A-K, Lemke JR, Pormann J, Schallner J, et al. Diagnostic value of partial exome sequencing in developmental disorders. *PloS One.* 2018;13(8):e0201041.
- 16 Mullegama SV, Jensik P, Li C, Dorrani N, UCLA Clinical Genomics Center, Kantarci S, et al. Coupling clinical exome sequencing with functional characterization studies to diagnose a patient with familial Mediterranean fever and MED13L haploinsufficiency syndromes. *Clin Case Rep.* 2017 Jun;5(6):833–40.
- 17 Thiffault I, Farrow E, Zellmer L, Berrios C, Miller N, Gibson M, et al. Clinical genome sequencing in an unbiased pediatric cohort. *Genet Med Off J Am Coll Med Genet.* 2019 Feb;21(2):303–10.
- 18 Gilissen C, Hehir-Kwa JY, Thung DT, van de Vorst M, van Bon BWM, Willemsen MH, et al. Genome sequencing identifies major causes of severe intellectual disability. *Nature.* 2014 Jul;511(7509):344–7.
- 19 Yamamoto T, Imaizumi T, Yamamoto-Shimojima K, Lu Y, Yanagishita T, Shimada S, et al. Genomic backgrounds of Japanese patients with undiagnosed neurodevelopmental disorders. *Brain Dev.* 2019 Oct;41(9):776–82.
- 20 Hamdan FF, Myers CT, Cossette P, Lemay P, Spiegelman D, Laporte AD, et al. High Rate of Recurrent De Novo Mutations in Developmental and Epileptic Encephalopathies. *Am J Hum Genet.* 2017 Nov;101(5):664–85.
- 21 Jiménez-Romero S, Carrasco-Salas P, Benítez-Burraco A. Language and Cognitive Impairment Associated with a Novel p.Cys63Arg Change in the MED13L Transcriptional Regulator. *Mol Syndromol.* 2018 Feb;9(2):83–91.
- 22 Martínez F, Caro-Llopis A, Roselló M, Oltra S, Mayo S, Monfort S, et al. High diagnostic yield of syndromic intellectual disability by targeted next-generation sequencing. *J Med Genet.* 2017 Feb;54(2):87–92.
- 23 Feng B-J. PERCH: A Unified Framework for Disease Gene Prioritization. *Hum Mutat.* 2017 Mar;38(3):243–51.
- 24 Quang D, Chen Y, Xie X. DANN: a deep learning approach for annotating the pathogenicity of genetic variants. *Bioinformatics.* 2015 Mar;31(5):761–3.
- 25 Rogers MF, Shihab HA, Mort M, Cooper DN, Gaunt TR, Campbell C. FATHMM-XF: accurate prediction of pathogenic point mutations via extended features. *Bioinforma Oxf Engl.* 2018 Feb;34(3):511–3.
- 26 Jagadeesh KA, Wenger AM, Berger MJ, Guturu H, Stenson PD, Cooper DN, et al. M-CAP eliminates a majority of variants of uncertain significance in clinical exomes at high sensitivity. *Nat Genet.* 2016 Dec;48(12):1581–6.

- 27 Chennen K, Weber T, Lornage X, Kress A, Böhm J, Thompson J, et al. MISTIC: A prediction tool to reveal disease-relevant deleterious missense variants. *PloS One*. 2020;15(7):e0236962.
- 28 Ioannidis NM, Rothstein JH, Pejaver V, Middha S, McDonnell SK, Baheti S, et al. REVEL: An Ensemble Method for Predicting the Pathogenicity of Rare Missense Variants. *Am J Hum Genet*. 2016 Oct;99(4):877–85.
- 29 McLaren W, Gil L, Hunt SE, Riat HS, Ritchie GRS, Thormann A, et al. The Ensembl Variant Effect Predictor. *Genome Biol*. 2016 Jun;17:122.
- 30 Hornbeck PV, Chabra I, Kornhauser JM, Skrzypek E, Zhang B. PhosphoSite: A bioinformatics resource dedicated to physiological protein phosphorylation. *Proteomics*. 2004 Jun;4(6):1551–61.
- 31 Lek M, Karczewski KJ, Minikel EV, Samocha KE, Banks E, Fennell T, et al. Analysis of protein-coding genetic variation in 60,706 humans. *Nature*. 2016 Aug;536(7616):285–91.
- 32 López-Ratón M, Rodríguez-Álvarez MX, Cadarso-Suárez C, Gude-Sampedro F. OptimalCutpoints: An R Package for Selecting Optimal Cutpoints in Diagnostic Tests. *J Stat Softw*. 2014 Nov;61(1):1–36.
- 33 Stieg DC, Willis SD, Ganesan V, Ong KL, Scuzo J, Song M, et al. A complex molecular switch directs stress-induced cyclin C nuclear release through SCFGrr1-mediated degradation of Med13. *Mol Biol Cell*. 2018 Feb;29(3):363–75.
- 34 Snijders Blok L, Hiatt SM, Bowling KM, Prokop JW, Engel KL, Cochran JN, et al. De novo mutations in MED13, a component of the Mediator complex, are associated with a novel neurodevelopmental disorder. *Hum Genet*. 2018 May;137(5):375–88.
- 35 Asadollahi R, Zweier M, Gogoll L, Schiffmann R, Sticht H, Steindl K, et al. Genotype-phenotype evaluation of MED13L defects in the light of a novel truncating and a recurrent missense mutation. *Eur J Med Genet*. 2017 Jun DOI: 10.1016/j.ejmg.2017.06.004
- 36 Hubisz MJ, Pollard KS, Siepel A. PHAST and RPHAST: phylogenetic analysis with space/time models. *Brief Bioinform*. 2011 Jan;12(1):41–51.
- 37 L. Daniels D. Mutual Exclusivity of MED12/MED12L, MED13/13L, and CDK8/19 Paralogs Revealed within the CDK-Mediator Kinase Module. *J Proteomics Bioinform*. 2013;01(S2). DOI: 10.4172/jpb.S2-004
- 38 Holt LJ. Regulatory modules: Coupling protein stability to phosphorylation during cell division. *FEBS Lett*. 2012 Aug;586(17):2773–7.
- 39 Malumbres M. Cyclin-dependent kinases. *Genome Biol*. 2014;15(6):122.
- 40 Tian Y, Pesaran T, Chamberlin A, Fenwick RB, Li S, Gau C-L, et al. REVEL and BayesDel outperform other in silico meta-predictors for clinical variant classification. *Sci Rep*. 2019 Sep;9(1):12752.

Figure legends

Figure 1: Comparison and correlations of meta-predictor algorithms. (A) ROC curve performances; (B) Correlation regarding all missense classifications; (C) Correlation regarding neutral missense classifications; (D) Correlation regarding pathogenic missense classifications.

Table 1: Evaluation of features for pathogenic and neutral missense variations

	Pathogenic (n = 38)	Neutral (n = 495)	significance
Grantham Score	94.50 [0.00 - 194.00]	58.00 [0.00 - 215.00]	$p=5.31e-4$
verPhyloP	5.19 [0.17 - 6.17]	3.04 [-0.84 - 6.32]	$p=1.14e-8$
verPhCons	1.00 [1.00 - 1.00]	0.93 [0.00 - 1.00]	$p=5.17e-3$
MED13 residue conservations	1.00 [0.00 - 1.00]	0.50 [0.00 - 1.00]	$p=2.95e-5$
Phosphorylation site distance	17.50 [0.00 - 263.00]	30.00 [0.00 - 321.00]	$p=2.95e-3$

Table 2: Performances of *in-silico* tools

	Thresholds	Se	Sp	PPV	NPV	MCC	ACC	AUC
BayesDel	0.234	0.757	0.913	0.400	0.980	0.492	0.902	0.877
CADD	25.10	0.842	0.717	0.186	0.983	0.308	0.726	0.810
DANN	0.995	0.676	0.658	0.132	0.964	0.174	0.660	0.691
FATHMM-XF	0.768	0.816	0.764	0.209	0.982	0.333	0.767	0.807
M-CAP	0.056	0.816	0.856	0.304	0.984	0.438	0.853	0.874
MISTIC	0.663	0.789	0.923	0.441	0.983	0.533	0.912	0.902
REVEL	0.634	0.789	0.893	0.361	0.982	0.484	0.886	0.873

ACC = Accuracy ; AUC = Area Under Curve ; MCC = Matthews Correlation Coefficient ; NPV = Negative Predictive Value ; PPV = Predictive Positive Value ; Se = Sensibility ; Sp = Specificity

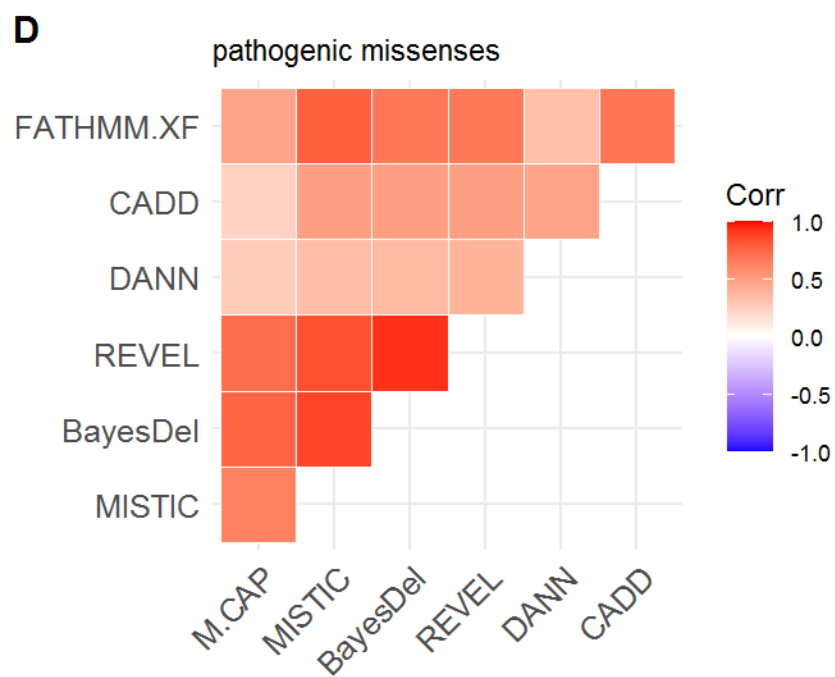
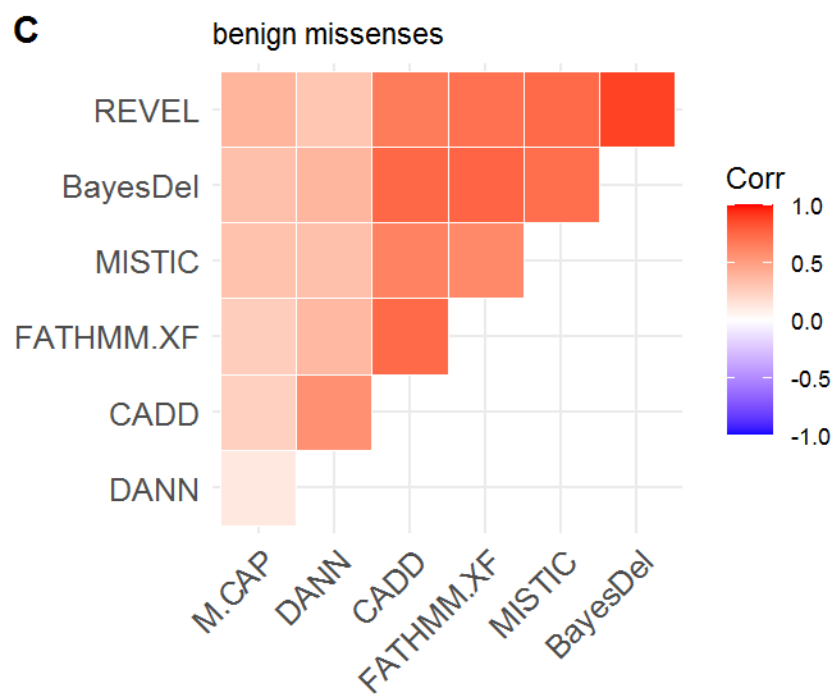
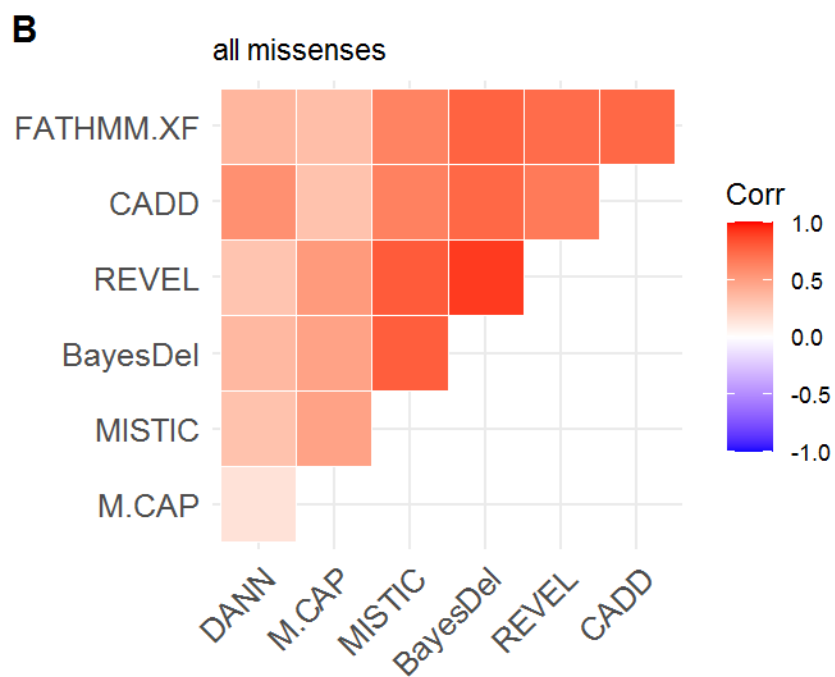
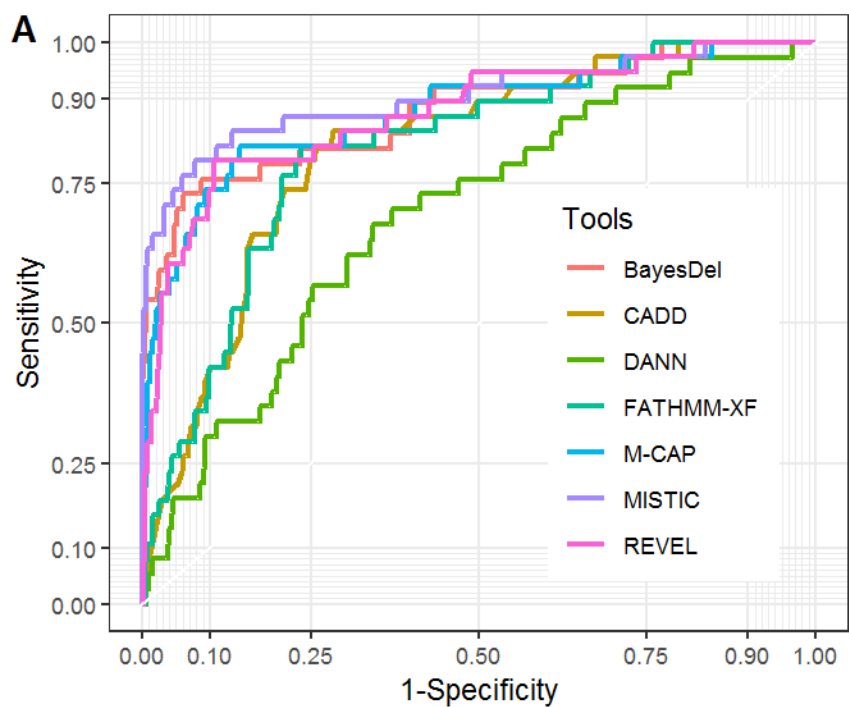


Table 1: Evaluation of features for pathogenic and neutral missense variations

	Pathogenic (n = 38)	Neutral (n = 495)	significance
Grantham Score	94.50 [0.00 - 194.00]	58.00 [0.00 - 215.00]	$p=5.31e-4$
verPhyloP	5.19 [0.17 - 6.17]	3.04 [-0.84 - 6.32]	$p=1.14e-8$
verPhCons	1.00 [1.00 - 1.00]	0.93 [0.00 - 1.00]	$p=5.17e-3$
MED13 residue conservations	1.00 [0.00 - 1.00]	0.50 [0.00 - 1.00]	$p=2.95e-5$
Phosphorylation site distance	17.50 [0.00 - 263.00]	30.00 [0.00 - 321.00]	$p=2.95e-3$

Table 2: Performances of *in-silico* tools

	Thresholds	Se	Sp	PPV	NPV	MCC	ACC	AUC
BayesDel	0.234	0.757	0.913	0.400	0.980	0.492	0.902	0.877
CADD	25.10	0.842	0.717	0.186	0.983	0.308	0.726	0.810
DANN	0.995	0.676	0.658	0.132	0.964	0.174	0.660	0.691
FATHMM- XF	0.768	0.816	0.764	0.209	0.982	0.333	0.767	0.807
M-CAP	0.056	0.816	0.856	0.304	0.984	0.438	0.853	0.874
MISTIC	0.663	0.789	0.923	0.441	0.983	0.533	0.912	0.902
REVEL	0.634	0.789	0.893	0.361	0.982	0.484	0.886	0.873

ACC = Accuracy ; AUC = Area Under Curve ; MCC = Matthews Correlation Coefficient ; NPV = Negative Predictive Value ; PPV = Predictive Positive Value ; Se = Sensibility ; Sp = Specificity